



## Molecular Crystals and Liquid Crystals Science and Technology. Section A. Molecular Crystals and Liquid Crystals

Publication details, including instructions for authors and subscription information:

<http://www.tandfonline.com/loi/gmcl19>

## Electronic Structure of a Stable Phenalenyl Radical as Studied by ESR/ENDOR, Paramagnetic NMR Spectroscopy and SQUID Measurements

Kozo Fukui<sup>a</sup>, Kazunobu Sato<sup>a</sup>, Daisuke Shiomi<sup>b</sup>, Takeji Takui<sup>a</sup>, Koichi Itoh<sup>b</sup>, Takashi Kubo<sup>c</sup>, Kosaburo Gotoh<sup>c</sup>, Kagetoshi Yamamoto<sup>c</sup>, Kazuhiro Nakasuji<sup>c</sup> & Akira Naito<sup>d</sup>

<sup>a</sup> Department of Chemistry, Graduate School of Science, Osaka City University, Sumiyoshi-ku, Osaka, 558-8585, Japan

<sup>b</sup> Department of Material Science, Graduate School of Science, Osaka City University, Sumiyoshi-ku, Osaka, 558-8585, Japan

<sup>c</sup> Department of Chemistry, Graduate School of Science, Osaka University, Toyonaka, Osaka, 560-0043, Japan

<sup>d</sup> Department of Life Science, Faculty of Science, Himeji Institute of Technology, Harima Science Garden City, Kamigori, Hyogo, 678-1297, Japan

Version of record first published: 24 Sep 2006

To cite this article: Kozo Fukui, Kazunobu Sato, Daisuke Shiomi, Takeji Takui, Koichi Itoh, Takashi Kubo, Kosaburo Gotoh, Kagetoshi Yamamoto, Kazuhiro Nakasuji & Akira Naito (1999): Electronic Structure of a Stable Phenalenyl Radical as Studied by ESR/ENDOR, Paramagnetic NMR Spectroscopy and SQUID Measurements, Molecular Crystals and Liquid Crystals Science and Technology. Section A. Molecular Crystals and Liquid Crystals, 334:1, 49-58

To link to this article: <http://dx.doi.org/10.1080/10587259908023302>

PLEASE SCROLL DOWN FOR ARTICLE

Full terms and conditions of use: <http://www.tandfonline.com/page/terms-and-conditions>

This article may be used for research, teaching, and private study purposes. Any substantial or systematic reproduction, redistribution, reselling, loan, sub-licensing, systematic supply, or distribution in any form to anyone is expressly forbidden.

The publisher does not give any warranty express or implied or make any representation that the contents will be complete or accurate or up to date. The accuracy of any instructions, formulae, and drug doses should be independently verified with primary sources. The publisher shall not be liable for any loss, actions, claims, proceedings, demand, or costs or damages whatsoever or howsoever caused arising directly or indirectly in connection with or arising out of the use of this material.

# Electronic Structure of a Stable Phenalenyl Radical as Studied by ESR/ENDOR, Paramagnetic NMR Spectroscopy and SQUID Measurements

KOZO FUKUI<sup>a</sup>, KAZUNOBU SATO<sup>a</sup>, DAISUKE SHIOMI<sup>b</sup>,  
TAKEJI TAKUI<sup>a</sup>, KOICHI ITOH<sup>b</sup>, TAKASHI KUBO<sup>c</sup>,  
KOSABURO GOTOH<sup>c</sup>, KAGETOSHI YAMAMOTO<sup>c</sup>,  
KAZUHIRO NAKASUJI<sup>c</sup> and AKIRA NAITO<sup>d</sup>

<sup>a</sup>Department of Chemistry, and, <sup>b</sup>Department of Material Science, Graduate School of Science, Osaka City University, Sumiyoshi-ku, Osaka 558-8585, Japan, <sup>c</sup>Department of Chemistry, Graduate School of Science, Osaka University, Toyonaka, Osaka 560-0043, Japan and <sup>d</sup>Department of Life Science, Faculty of Science, Himeji Institute of Technology, Harima Science Garden City, Kamigori, Hyogo 678-1297, Japan

We have studied magnetic properties and electronic structures of a novel persistent neutral radical, 2,5,8-tri-*tert*-butylphenalenyl(**2**), which is the first example of alternant hydrocarbon  $\pi$ -radical isolated in the crystalline state. The observed magnetic susceptibilities of polycrystalline sample **2** were reproduced by assuming the thermal equilibrium between singlet ground state and excited triplet state of the dimer ( $2J/k_B = -2 \times 10^3$  K) with traces of paramagnetic impurity molecules (0.3 mol%). The  $\pi$ -spin density distribution of radical **2** was determined by liquid-phase cw-ESR, <sup>1</sup>H-ENDOR/TRIPLE, and paramagnetic <sup>1</sup>H-NMR measurements. The origin of the large inter-molecular antiferromagnetic interaction in the crystal **2** was explained by an occurrence of effective SOMO-SOMO overlap between the two radicals on the six equivalent  $\alpha$ -positions with large positive spin densities of the carbon sites.

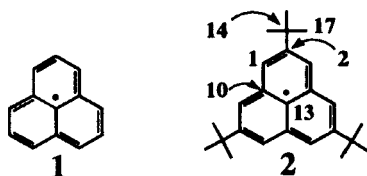
**Keywords:** persistent phenalenyl radical; magnetic susceptibility; ENDOR/TRIPLE; paramagnetic NMR; spin density distribution; pancake bonding

## INTRODUCTION

After the discovery of the first purely organic ferromagnet, *p*-NPNN in 1991<sup>[1,2]</sup>, increasing attention has been paid to the solid-state properties of organic free radicals in the rapidly developing research field of organic magnetics/molecule-based magnetism. Neutral radicals, in particular, nitroxide and

nitronyl nitroxide family have extensively been studied so far because these materials have excellent stability and good crystallinity. Turning our attention to a series of neutral hydrocarbon  $\pi$ -radicals, we realize that any stable single crystal composed of the  $\pi$ -radical molecules fit for X-ray structure analysis has not been obtained except for the only one example, pentaisopropylcyclopentadienyl<sup>[3]</sup>. In spite of the difficult chemical isolation, the crystals composed of neutral hydrocarbon  $\pi$ -radicals can be considered as more fundamental systems because they are free from charges, counter ions, and heteroatomic effects that make their solid-state properties more complicated.

Phenalenyl (1) is a well-known odd-alternant hydrocarbon  $\pi$ -radical ( $S=1/2$ ) which has both high symmetry ( $D_{3h}$ ) and high stability in solution<sup>[4]</sup>. It was recently isolated as solvent-free pure radicals in the crystalline state by introducing *tert*-butyl groups into 2-, 5- and 8-positions of the phenalenyl skeleton<sup>[5]</sup>. The X-ray structure analysis of the crystal of 2,5,8-tri-*tert*-butylphenalenyl (2) showed that molecules 2 are dimerized in the monoclinic



crystal ( $P2_1/n$ ,  $Z=4$ ) (Fig. 1)<sup>[5]</sup>. The two planar radicals 2 face each other in the dimer, where one is related to the other by an inversion symmetry. The mean inter-plane distance is about  $3.30\text{\AA}$ , which is smaller than the corresponding van der Waals contact ( $3.4\text{--}3.5\text{\AA}$ ), suggesting that a large antiferromagnetic interaction occurs between the  $S=1/2$  monomer radicals due

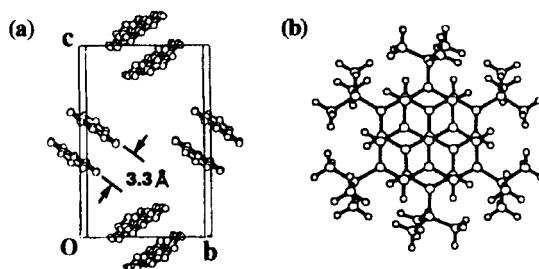


FIGURE 1 (a) Packing diagram of crystal 2. *Tert*-butyl groups are omitted for clarity. (b) Molecular structure of the dimer.

to an orbital overlap.

In this paper, we first describe the magnetic properties of the crystal **2** by SQUID measurements. It is essential to investigate the monomer radical **2** in solution because its electronic spin structure offers an insight into the magnetic properties of the dimer structure. Then, we have performed liquid-phase cw-ESR, <sup>1</sup>H-ENDOR/TRIPLE and paramagnetic <sup>1</sup>H-NMR measurements in order to determine the  $\pi$ -spin density distribution of radical **2**. The origin of the strong intermolecular antiferromagnetic interaction within the dimer is discussed in terms of MO calculation.

## EXPERIMENTAL

The static magnetic susceptibility of radical **2** in the crystalline state was measured for the polycrystalline sample using a Quantum Design MPMS2 SQUID magnetometer with an applied field of 0.2 T in the temperature range of 1.8–300K. The diamagnetic susceptibility, which could not be calculated from Pascal's sum rule because of its unique structure of ring currents<sup>[6]</sup>, was estimated to be  $-235.3 \times 10^{-6} \text{ emu mol}^{-1}$  and was subtracted. The liquid-phase cw-ESR, <sup>1</sup>H-ENDOR/TRIPLE spectra of radical **2** were recorded in toluene solution ( $1.8 \times 10^{-5} \text{ M}$ ) at 290K on an X-band Bruker ESR/ENDOR spectrometer ESP300/380E. The paramagnetic <sup>1</sup>H-NMR spectra of **2** were taken in CDCl<sub>3</sub> solution (0.24M) at 300K on a Varian NMR spectrometer UNITY-500. The samples were degassed and sealed on a vacuum line by several freeze-pump-thaw cycles before the measurements.

## RESULTS AND DISCUSSION

### Magnetic Susceptibility

Fig. 2 shows the temperature dependence of  $\chi T$  (the product of paramagnetic susceptibility  $\chi$  and temperature  $T$ ), in which one can recognize that a small amount of  $\chi T$  was observed and remained constant below 200K, following the Curie law. This contribution corresponding to about 0.3mol% of total radical concentration is ascribable to paramagnetic impurity molecules. The  $\chi T$  values exhibited a gradual increase on raising the temperature above 200K. It arises from a growing population of thermally accessible triplet state of the dimers. Assuming the singlet-triplet model, the  $\chi T$  curve was reproduced

using the well-known Bleaney-Bowers equation Eq. (1)<sup>[7]</sup>,

$$\chi = (Ng^2\mu_B^2 / k_B T) / [3 + \exp(-2J/k_B T)]. \quad (1)$$

The energy separation  $2J/k_B$  was determined to be  $2 \times 10^3 \text{ K}$ .

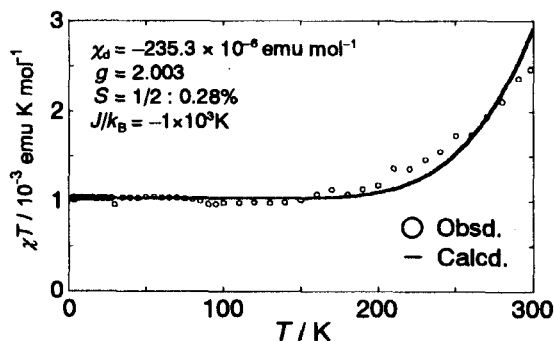


FIGURE 2 Temperature dependence of  $\chi T$  (the products of paramagnetic susceptibility and temperature) of radical **2** in the crystalline state.

### ESR Spectra

The liquid-phase cw-ESR spectrum of **2** exhibited hyperfine structure characteristic of six equivalent ring protons, while hyperfine splittings due to 27 methyl protons are too small to be resolved in the spectrum (Fig. 3). Moreover,  $^{13}\text{C}$  satellite signals corresponding to natural abundance (1.1%) were clearly observed at the both sides of main peaks<sup>[8]</sup>. We determined all the

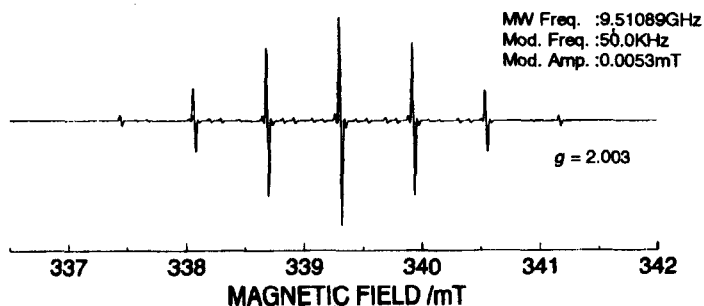


FIGURE 3 Observed ESR spectrum of **2** in toluene solution at 290 K.

hyperfine coupling constants (hfcc's) of  $^{13}\text{C}$  nuclei with the help of spectrum simulation using the program *Simfonia* by Bruker Instruments, Inc.

### **$^1\text{H}$ -ENDOR/TRIPLE Spectra**

For doublet ( $S=1/2$ ) species, ENDOR signals with the hfcc value of  $|a_{\text{H}}(i)|$  smaller than  $2\nu_{\text{H}}$  appear at

$$\nu_{\pm} = \nu_{\text{H}} - a_{\text{H}}(i) m_{\text{S}}/\hbar = \nu_{\text{H}} \pm a_{\text{H}}(i)/2\hbar \quad (m_{\text{S}} = -1/2 \text{ or } +1/2), \quad (2)$$

where  $\nu_{\text{H}}$  stands for the free proton NMR frequency. The hfcc  $|a_{\text{H}}(i)|$  is determined from the separation between a pair of the ENDOR transitions at  $\nu_{\pm}$ .

Fig. 4(a) shows that two pairs of  $^1\text{H}$ -ENDOR signals were found for a toluene solution of **2** at 290K by monitoring the most intense central ESR line at 339.3 mT in Fig. 3. The inner pair of the signals, however, is apparently a single line as a result of their superposition due to the small hfcc.

$$|a_{\text{H}}(1)| = 17.365 \text{ MHz} = 0.6195 \text{ mT}, \quad (3)$$

$$|a_{\text{H}}(17)| < 0.14 \text{ MHz} (< 0.0050 \text{ mT}). \quad (4)$$

The TRIPLE transitions belonging to the same  $m_{\text{S}}$ -manifold ( $m_{\text{S}}=+1/2$  or  $-1/2$  for a doublet radical) as that of an RF-pumped transition diminish their intensity, while those belonging to another  $m_{\text{S}}$ -manifold gain their intensity. From the assignment of  $m_{\text{S}}$  together with the relation in Eq. (2), the relative

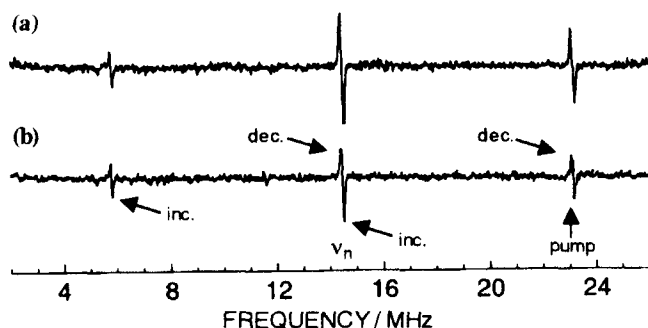


FIGURE 4 Liquid-phase (a)  $^1\text{H}$ -ENDOR and (b)  $^1\text{H}$ -TRIPLE spectra of **2** observed in toluene solution at 290K.  $\nu_{\text{H}}$  indicates the free proton NMR frequency. "inc." and "dec." denote the increase and the decrease in signal intensity, respectively.

signs of  $hfcc$ 's,  $a(i)$ 's, can be determined in TRIPLE measurements.

Fig. 4(b) shows a general  $^1\text{H}$ -TRIPLE spectrum of **2** obtained by pumping the ENDOR transition of ring protons at 23.129MHz, where the pump frequency gives a slight but discernable distortion to the lineshape of the central line. It enables us to determine the relative signs of  $hfcc$ 's,  $a_{\text{H}}(1)$  and  $a_{\text{H}}(17)$ , to be opposite with each other.

### Paramagnetic $^1\text{H}$ -NMR Spectra

The NMR spectroscopy for organic free radicals provides a means of determining both the sign and the magnitude of small  $hfcc$ 's which can not be acquired by ESR/ENDOR measurements<sup>[9]</sup>. A sufficient condition for observing a single shifted NMR line for each group of equivalent nuclei is that either:

$$T_1^{-1} \gg a(i), \quad (5)$$

or

$$T_e^{-1} \gg a(i). \quad (6)$$

In these inequalities  $T_1$  is the paramagnetic relaxation time and  $T_e$  is a time characterizing electron exchange. For concentrated solutions of organic free radicals, spin exchange may be rapid enough so that the above condition is fulfilled.

A broad NMR signal was observed for a deuteriochloroform solution of radical **2** (0.24M) at 300K as shown in Fig. 5. A paramagnetic shift,  $-\Delta H/H_0$ , was given by a difference between a signal of methyl protons of radical **2** and that of the diamagnetic precursor, 2,5,8-tri-*tert*-butylphenalen<sup>[5]</sup>.

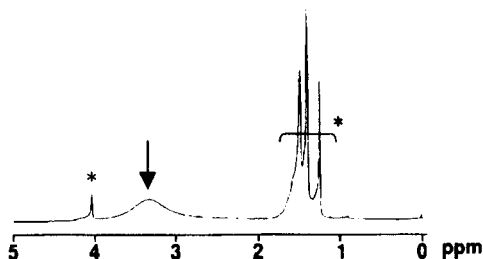


FIGURE 5 Paramagnetic  $^1\text{H}$ -NMR spectrum of **2** observed in  $\text{CDCl}_3$  solution at 300K. The solid arrow indicates the signal due to methyl protons. Asterisks denote the signals by diamagnetic impurity molecules.

TABLE I Isotropic hyperfine coupling constants (/mT) of **2**.

	$a_H(1)$	$a_H(17)$	$a_C(1)$	$a_C(2)$	$a_C(10)$	$a_C(13)$	$a_C(14)$	$a_C(17)$
ESR	(-)0.620	—	(+)0.964	(-)0.780	(-)0.780	(+)0.320	0.070	0.071
ENDOR	-0.6195	+δ	—	—	—	—	—	—
NMR	—	+0.0026	—	—	—	—	—	—

$$-\Delta H/H_0 = 3.309 \text{ ppm} - 1.375 \text{ ppm} = +1.934 \text{ ppm.} \quad (7)$$

The paramagnetic shift is proportional to the hfcc  $a_H(i)$  as

$$-\Delta H/H_0 = (\gamma_e / \gamma_N) (g\mu_B / 4k_B T) \cdot a_H(i). \quad (8)$$

The hfcc  $a_H(17)$  was determined to be +0.0026 mT by Eq. (8).

#### Determination of $\pi$ -Spin Density Distribution

The obtained hfcc's are summarized in Table I. The  $\pi$ -spin densities ( $\rho$ 's) of the 1- and 14-positions are calculated from the observed hfcc's by assuming that McConnell equation,

$$a_H(1) = Q_1 \rho_1, \quad (Q_1 = -2.87 \text{ mT}^{10-12}) \quad (9)$$

and a relationship of hyperconjugation effect for methyl group,

$$a_H(17) = Q_2 \rho_{14}, \quad (Q_2 = +2.00 \text{ mT}^{13}) \quad (10)$$

can hold for the electron system of **2**, being determined as follows;

$$\rho_1 = +0.216, \quad \rho_{14} = +0.0013. \quad (11)$$

In order to determine the  $\pi$ -spin densities on the other carbon sites with no neighboring proton, the empirical equations proposed by Karplus *et al.* were applied, where the spin densities on the neighboring carbon atoms are taken into account<sup>[14]</sup>. In the present case, the equations for each carbon site of radical **2** are as follows,

$$a_C(1) = 3.56 \rho_1 - 1.39 (\rho_2 + \rho_{10}), \quad (12)$$

$$a_C(2) = Q \rho_2 - 1.39 (2\rho_1 + \rho_{14}), \quad (13)$$

$$a_C(10) = 3.05 \rho_{10} - 1.39 (2\rho_1 + \rho_{13}), \quad (14)$$

$$a_C(13) = 3.05 \rho_{13} - 1.39 (3\rho_{10}), \quad (15)$$

where new parameters,  $Q$  and  $\rho_{14}$ , were introduced in Eq.(13) for considering the contribution from a neighboring  $sp^3$  carbon site. The substitution of the experimental values for  $\rho_1$ ,  $\rho_{14}$  and  $a_c(i)$ 's yielded the  $\pi$ -spin densities on each site as shown in Fig. 6.

The experimentally determined  $\pi$ -spin density distribution shows that large positive spin densities occur at the six equivalent  $\alpha$ -positions of radical **2** as expected from the simple HMO theory. Moreover, an intramolecular  $\pi$ -spin polarization effect dominates, giving rise to the successive alternation of the signs of  $\pi$ -spin densities among the carbon sites neighboring with each other.

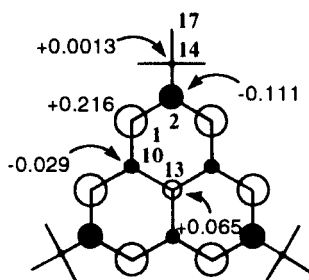


FIGURE 6 Experimentally determined  $\pi$ -spin density distribution of **2**.

### **Electronic Structure of the Radical Dimer in Crystal**

The singlet-dimer structure in the crystal is explained by both the  $\pi$ -spin density distribution and the molecular packing of the dimer with  $D_{3d}$  symmetry. The packing results in an occurrence of effective  $\pi$ - $\pi$  overlap between the singly occupied molecular orbitals (SOMOs) on the six equivalent  $\alpha$ -positions with the large positive spin densities as shown in Fig. 7.

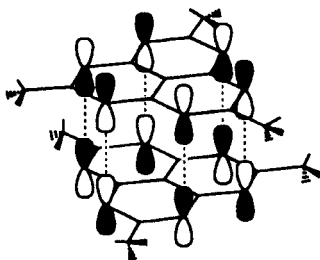


FIGURE 7 Schematic representation of the effective SOMO-SOMO overlap.

According to a simple  $\pi$ -MO calculation, it turns out that frontier molecular orbitals are generated from the  $\pi$ - $\pi$  interaction between the two SOMOs of the paramagnetic monomers (Fig. 8). The formation of singlet-dimer and its electronic structure are well understood in terms of a supermolecule approach. Two unpaired electrons are accommodated in the super-HOMO of the dimer, giving rise to a spin cancellation and bond formation between the monomers.

The broad CT band observed at 612nm in solid<sup>[5]</sup> corresponds to the excitation from the super-HOMO to the super-LUMO. According to the group theoretical argument, the CT transition ( $a_{2g} \leftarrow a_{1u}$ ) is allowed only in the direction perpendicular to the molecular plane of the two fragments. The transition moment of the CT band was confirmed to be polarized in the CT reflection band observed in the crystalline state<sup>[5]</sup>, being in good agreement with the above model.

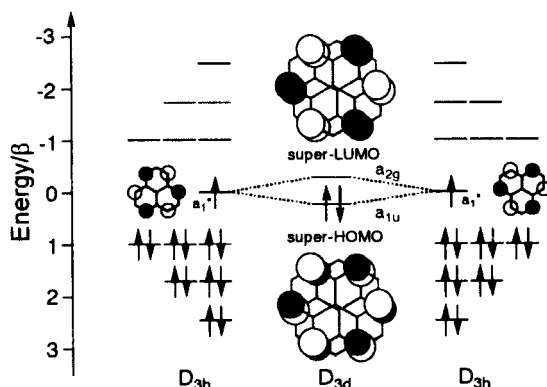


FIGURE 8 MO diagram of the dimer (Supermolecule).

## CONCLUSION

We have examined a persistent neutral hydrocarbon  $\pi$ -radical, 2,5,8-tri-*tert*-butylphenalenyl (**2**) by SQUID measurements, liquid-phase cw-ESR, <sup>1</sup>H-ENDOR/TRIPLE, and paramagnetic <sup>1</sup>H-NMR spectroscopy. The  $\pi$ -dimer structure clarified by X-ray analysis was confirmed by the observed magnetic susceptibility, which was described by a ground-state singlet dimer model with

$2J/k_B = -2 \times 10^3 \text{ K}$ . This strong intermolecular antiferromagnetic interaction can be well explained in terms of both the crystal packing of **2** and the  $\pi$ -spin density distribution experimentally determined, which ensure the occurrence of effective  $\pi$ - $\pi$  overlap between the two SOMOs in the crystal. The crystal of **2** is a fundamental system that consists solely of neutral genuine hydrocarbon  $\pi$ -radicals. It is an example where multi-centered  $\pi$ - $\pi$  bonding (or, "pancake bonding" by Mulliken) are found between neutral organic radicals.

## References

- [1] M. Tamura, Y. Nakazawa, D. Shiomi, K. Nozawa, Y. Hosokoshi, M. Ishikawa, M. Takahashi, and M. Kinoshita, *Chem. Phys. Lett.*, **186**, 401 (1991).
- [2] Y. Nakazawa, M. Tamura, N. Shirakawa, D. Shiomi, M. Takahashi, M. Kinoshita, and M. Ishikawa, *Phys. Rev. B*, **46**, 8906 (1992).
- [3] H. Sitzmann, H. Bock, R. Boese, T. Dezember, Z. Havlas, W. Kaim, M. Moscherosch, and L. Zanathy, *J. Am. Chem. Soc.*, **115**, 12003 (1993).
- [4] (a) D. H. Reid, *Quart. Rev.*, **19**, 274 (1965). (b) K. Ohashi, T. Kubo, T. Masui, K. Yamamoto, K. Nakasuji, T. Takui, Y. Kai, and I. Murata, *J. Am. Chem. Soc.*, **120**, 2018 (1998).
- [5] K. Nakasuji *et al.*, *J. Am. Chem. Soc.*, submitted.
- [6] I. Sethson, D. Johnels, and U. Edlund, *J. Chem. Soc. Perkin Trans. 2*, 1339 (1990).
- [7] R.L. Carlin, *Magnetochemistry* (Springer-Verlag: New York, 1986) p.75.
- [8] The ESR measurements with lower field-modulation confirmed that these signals are not sideband formation.
- [9] G.N. La Mar, W.D. Horrocks Jr., R.H. Holm, *NMR of Paramagnetic Molecules* (Academic Press 1973) chap. 15.
- [10] The  $Q_j$  value used here is that for non-substituted phenalenyl radical, which was determined by McConnell equation using both the experimental hfcc value by ENDOR measurement and the estimated spin density by UHF calculation, which are described in references [11.] and [12.], respectively.
- [11] B. Kirste, and H. Kurreck, *Appl. Spectrosc.*, **34**, 305 (1980).
- [12] S.H. Glarum, and J.H. Marshall, *J. Chem. Phys.*, **44**, 2884 (1966).
- [13] C. Heller, and H.M. McConnell, *J. Chem. Phys.*, **32**, 1535 (1960).
- [14] M. Karplus, and G.K. Fraenkel, *J. Chem. Phys.*, **35**, 1312 (1961).